AFDEX Newsletter
Q1 / 2023

MFRC
www.afdex.com, mfrc@afdex.com
Tel: +82-55-755-7529, Fax: +82-55-761-7529

Contents

1. AFDEX_V23R01 & Revised Version of AFDEX_V21 Release

AFDEX_V21R03 was released on May 12th, 2022. It offers a new set of improvements in solver and Pre/Postprocessors, which are described in Sections 2 and 3. AFDEX_V23, the next version is planned to be released in March 2023.

2. AFDEX_V23R01 Improvements

2.1 Temperature Compensation of Cylinder Compression Testing

A specimen experiences the increase in temperature due to plastic deformation and barreling due to friction during the compression testing. The initial flow curve information obtained from the testing under the assumption of isothermal condition and homogeneous compression is different from the actual flow information depending on flow behavior, coefficient of heat transfer, heat capacity, etc.

Figure 2.1 shows the experimental flow curve obtained from the compression testing of AZ91E Mg alloy (solid lines) and its fitted curves with/without considering the temperature-compensation.

Experimentally, the friction does not affect much on results of cylinder compression testing. The minimized friction during the testing is one of the reasons. The major reason lies in the fact that the restrained contact area between the tool and material compensates for the increased flow stress due to deformation inhomogeneity, which are both caused from the barreling, that is, the effect of friction at the contact interface.

The results of the compression testing conducted by using the flow curves in Figure 2.1 describe that the difference between the experimental and predicted compression loads is large. (Refer to non-temperature-compensated curve in Figure 2.2).

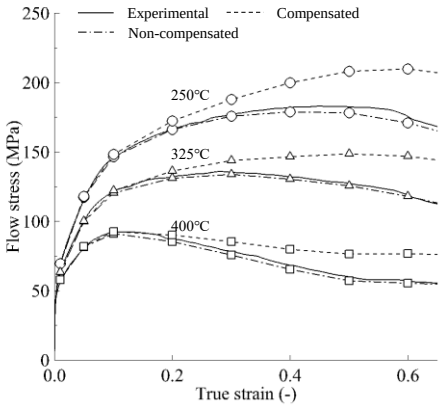

Figure 2.1 AZ31B (Strain rate = 20 1/s)

There is no significant difference between the experiment of the compression testing (Solid lines in Figure 2.2) and its prediction used the temperature-compensated flow curve (broken lines in Figure 2.2), which the mean error is about 3.2%.

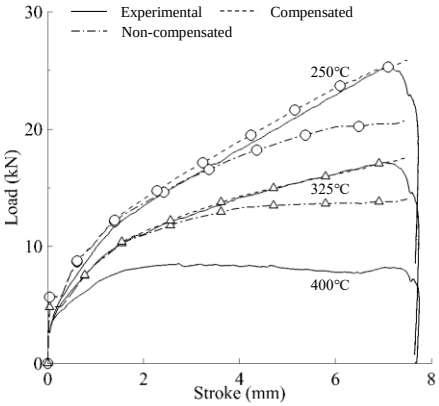

Figure 2.2 Comparison between experiment and prediction of compression testing

Figure 2.3(a) compares the analysis results using the temperature-compensated flow information with the experimental results, which shows that the effect of the temperature compensation is not large in terms of the shape prediction. On the other hand, the forming load has a significant difference in Figure 2.3(b). The maximum forming load obtained through the experiment was 9.48 MN. The forming load predicted by the temperature-compensated flow information is 9.00 MN (95% of the experimental value), while that obtained by the temperature-compensated flow information is 7.11 MN (75% of the experimental value).

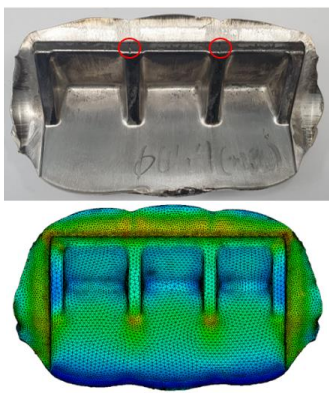

(a) Deformed shape

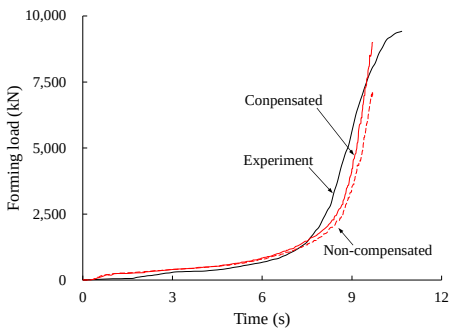

(b) Comparison of forming load

Figure 2.3 Comparison of analysis results and experimental results

2.2 Direct Method for Calculating Peak Strain

Peak strain and 50% strain are required for the prediction of the microstructure during hot forging. The traditional way of calculating peak strain is to use the closed-form function of strain, strain rate, temperature, etc. The weak point of this function is to lead to a large error.

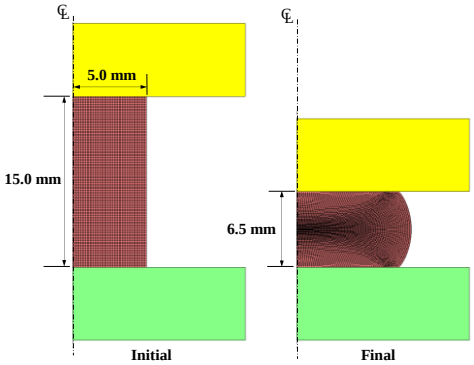

Figure 2.4 Application (Upsetting process)

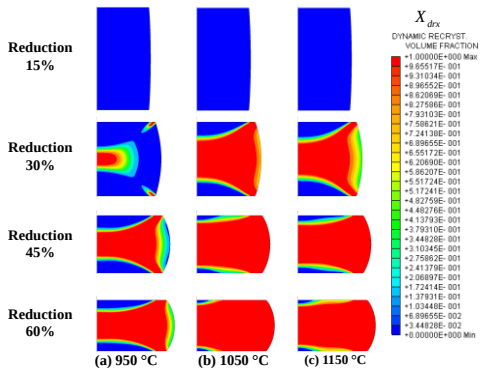

(a) Distribution of Xdrx

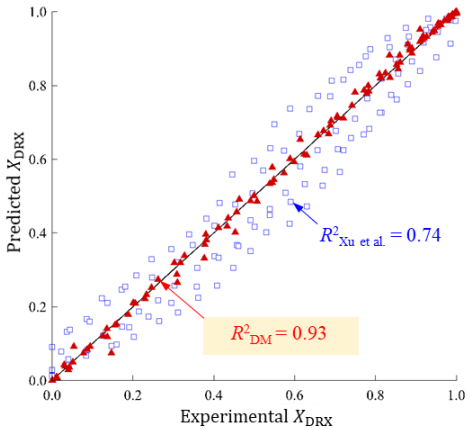

(b) Result accuracy (Red mark: Direct method)

Figure 2.5 Comparison between predicted and experimental results

Also, it is challenging process to find the function for calculating peak strain because it varies depending on a material due to the fact that flow curve (or flow function) is affected sensitively by the function. Therefore, this is deficient in prediction of microstructure evolution.

Recently, AFDEX has become supported by a high precision description of flow curves. With the accurate formulation of the flow curve, we can develop a direct method of acquiring peak strain and 50% strain directly from the flow functions, where were already constructed in the material database for flow analysis. Figure 2.4 defines the application example of the direct method to predict the microstructural evolution.

Figure 2.5(a) depicts the distribution of Xdrx. As shown in Figure 2.5(b), the predicted result shows good agreement with the experimental data. (Red mark: AFDEX data obtained by the direct method, Blue mark: Reference). The result from the data reveals that the predicted grain size is 46.3μm, and the mean error is 2.7%. A detailed information on this will be provided in the paper scheduled to be published shortly (M. S. Joun et al., 2022, J. Mater. Res. Technol. V. 18, pp. 3894-3907).

2.3 Double Curvature Strain Hardening

Figure 2.6 highlights that a tensile testing result of stainless steels has strain hardening with double curvature in the case when engineering strain at the necking point is large while the strain difference between the necking point and the fracture point is relatively small.

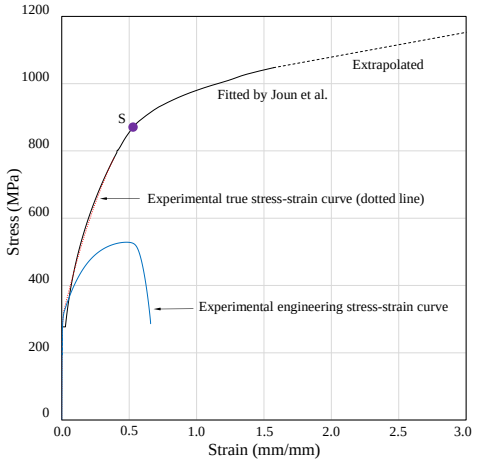

Figure 2.6 Tensile curve and flow curve of SUS 304 at room temperature

Recently, this flow behavior has been investigated by some researchers. It is impossible to express such double strain hardening flow behavior using the conventional flow stress model.

AFDEX research team have developed the Voce-Ludwik strain hardening flow model based on the extreme curvature strain for an effective description of the double curvature strain hardening behavior. Figure 2.7 compares the flow curve obtained using the proposed model with the result of tensile testing. It is important to formulate a more accurate flow model for high-strength steels.

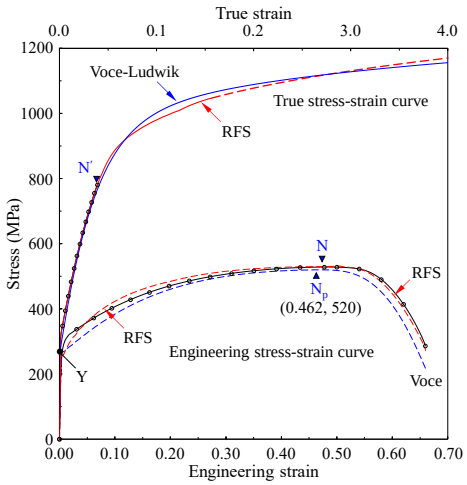

Figure 2.7 Comparison between experimental and fitted flow curves and their corresponding tensile testing

2.4 Automatic Simulation of Pilger Rolling Process

Pilger rolling process is a special metal forming process that can manufacture long tubes of difficult-to-form materials including stainless steels, ziraloys, etc. with great areal reduction at a single stage. This is one of incremental metal forming methods, which involves rolling, extrusion, upsetting, etc. Pilgering process is friendly to mass production of high-quality pipes as well as automation and environment. Therefore, the conventional drawing processes for metallic tubes will be possibly replaced by this pilgering processes in gradual. The pilgering process is characterized by the three-dimensional rolls which not only rotates but also moves back and forth at once and the fixed mandrel which forms and controls the internal surface of the tubes. The material periodically moves and rotates.

Especially, there should be a huge difference in product quality between the pilgered and drawn tubes because the materials during pilgering process experience plastic deformation owing to compressive load. To the contrary, the materials in the conventional drawing processes experience both tensile and compressive plastic deformation.

Recently, AFDEX provides the fully automatic simulation of the pilgering processes covering both single and composite materials. The fully automatic simulation is available using either rigid-plastic FEM or implicit elastoplastic FEM by entering the inputs involving feed rate, rotation angle, etc. A special mesh system with layers in the thickness direction is available.

Figure 2.8 shows the analysis results of the example from a reference. The simulation was fully-automatically conducted.

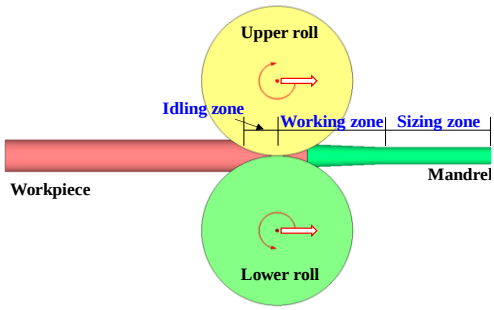

(a) Process definition

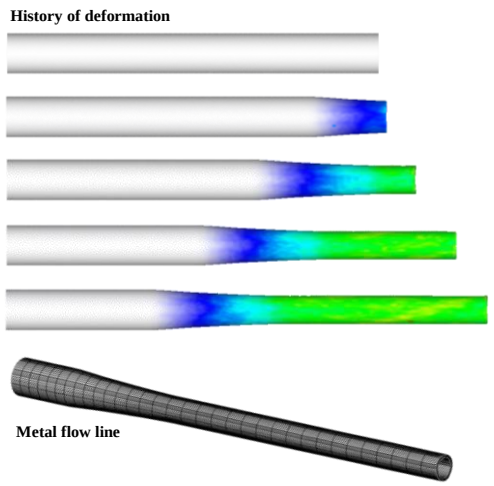

(b) Deformed shape, effective stress distribution, and metal forming

Figure 2.8 Analysis results of Pilger rolling process

2.5 Local Material-Motion Constraining Function and its Application

The analysis of the ring rolling process is exposed to the problem of an extremely small contact surface compared to the volume of the material. Since the material is not trapped like forging, it has a difficult problem of predicting the deformed shape with accuracy. Since the work roll and the material are in contact with the outside in two circles, the smooth contact condition cannot be achieved in the finite element simulation. In this case, it is difficult to impose frictional condition accurately that controls the spread. From an empirical point of view, the finite element model is close to the line contact between the work roll and the material, and the actual spread of the ring material is not much. Due to these problems, there is a limit to solving the ring rolling simulation problem with the existing friction law. If the function of artificially controlling the motion of the material in the contact area is used, the strength of the control of the material can be adjusted by the user, so it is possible to solve the above problem in an engineering way instead of the existing friction laws.

Figure 2.9(a) defines the application region of this function. If this function is not applied, the side wall is inclined as shown in Figure 2.9(b). This is the result that the outer surface of the ring material receives resistance to spreading by the step of the work roll as the spread increases, but the material on the mandrel side does not receive that resistance. On the other hand, when this function is applied, as shown in Figure 2.9(c), the side of the ring becomes close to the vertical line. This function is quantitatively evaluated to replace the friction law in the process analysis of the ring rolling process in the future.

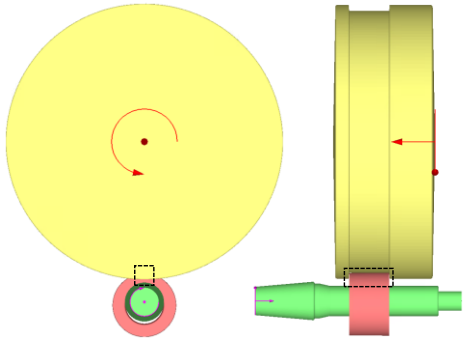

(a) Applied region

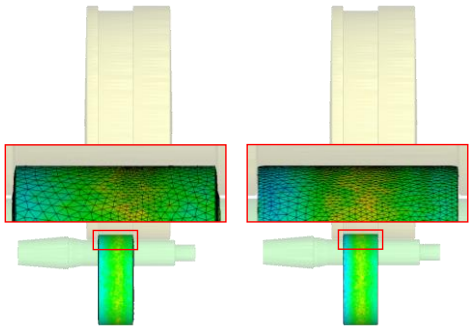

(b) Not applied (c) Applied

Figure 2.9 Profile ring rolling process simulation using new function

2.6 Boss Forming Simulation

Multi-body elastoplastic finite element analysis technology which has been provided from AFDEX_V21 is essential for analytical purposes of special processes, including not only for multi-body structural analysis and metal forming simulation but also for the FE analysis of special mechanical problems where the die control is greatly affected by plastic deformation of the material. Here, we introduce a 2D example among the recently applied examples.

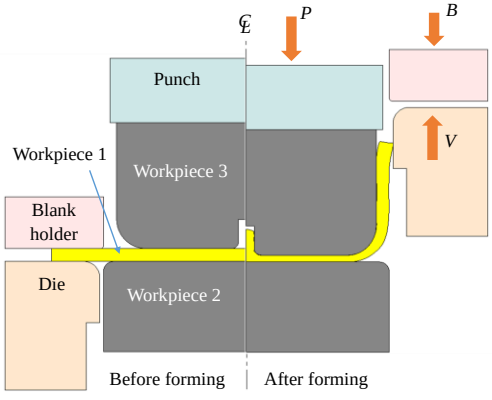

(a) Conceptual drawing of the boss forming process

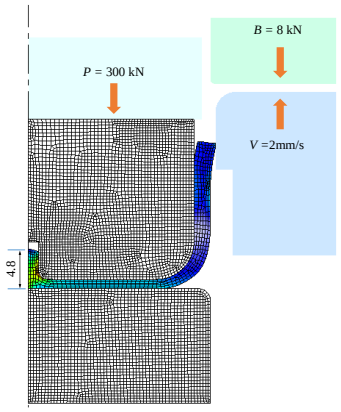

(b) FE prediction

Figure 2.10 Elastoplastic finite element analysis of the boss forming process using multi-body function

Figure 2.10(a) shows the boss forming process in which the upper punch and right upper binder (blank holder) apply the given forces on the sheet or plate material and the lower punch and right lower die support and push the material with zero and given velocities, respectively. Mechanically, it is summarized that the binder and the movable lower die gradually strengthen the conditions of plastic deformation by applying radial stress to the material between the upper and lower punches. Figure 2.10(b) is the FE prediction of the test boss forming process predicted under the following conditions: P = 300kN, friction coefficient = 0.07 and B = 8kN. The predicted ratio of the boss height to the initial sheet thickness (h/t) is 4.8/2.0, which is similar to the work of Wang et al. (CIRP Annals-Manuf. Technol., V. 62, 291-294, 2013). Note that the B value was assumed in this simulation.

2.7 Simulation of Tube Drawing Process with Nonuniform Thickness and Die Misalignment

FE analyses of tube drawing processes have traditionally been conducted under the assumptions of uniform thickness of the mother tube, fixed mandrels, and right alignment of dies or tools. Analysis results obtained under such assumptions have very limited meaning.

Actual mother tube allows thickness variation within 10%. Therefore, the change in thickness variation caused by the plastic deformation during tube extrusion is a major concern. Figure 2.11 shows the tube drawing process with a mother tube with non-uniform thickness and a die inclined at 5 degrees with an emphasis on the multi-body implicit elastoplastic finite element mode. The characteristic of this process is that the mandrel is automatically positioned properly to balance the load as shown in the Figure 2.11. That is, the initial position of the mandrel is located at the center but moved to a point where the mechanical balance was achieved with the progress of the process simulation. The FE predictions of this process showed a similar trend to the experimental works done by N. Al-Hamdany et al. (Tube drawing with tilted die: Texture, dislocation density and mechanical properties," Metals, Vol. 11, 2021) in terms of thickness deviation. According to the FE predictions, the thickness deviation can be improved or worsened depending on the direction of the inclination angle of the die.

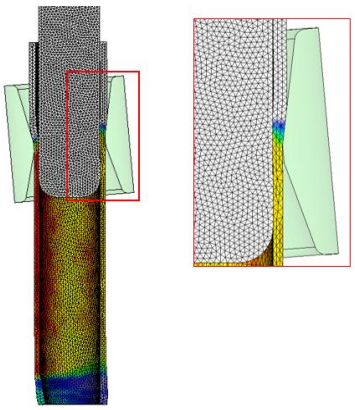

Figure 2.11 Simulation of assymmetric extrusion process

2.8 Quenching & Tempering Simulation of Jominy Testing

The degree of hardness decrease is determined by the maintainance temperature and time during tempering. Figure 2.12(b) shows the phase fraction during the heat treatment predicted using the TTT curve in Figure 2.12(a). At the end of quenching, 90% of austenite is converted to perlite, bainite, and finally martensite. This quenching induced phase transformation and thermal expansion and contraction owing to the quenching and/or tempering cause the deformation and volumetric change of the material. Figure 2.12(c) shows an example of predicting them.

This feature regarding the heat treatment is planned to be released in March 2023 through the beta version of AFDEX_V23.

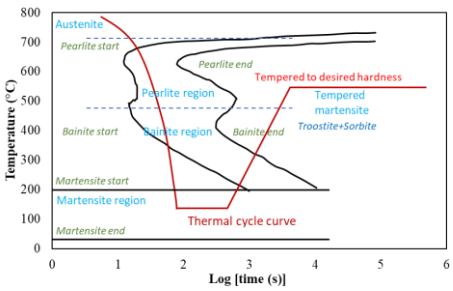

(a) TTT-curve

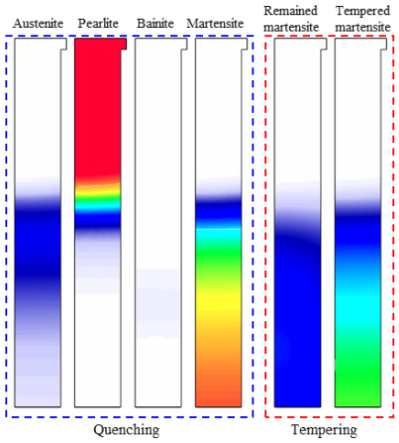

(b) Volume phase fraction

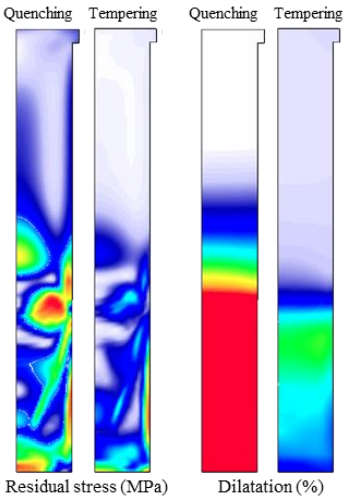

(c) Distortion analysis

Figure 2.12 Heat treatment analysis

3. Pre/Post-processor Improvements

3.1 Automatic Mesh Density Control for 3D Dies

Previously, heat transfer analysis during nonisothermal (coupled) analysis and die structural analysis has been conducted using common mesh systems without any mesh density control. Now, AFDEX_V21R03 provides the feature of automatic mesh density control which can find a core of a die. This feature can help user to skip the procedure for applying the region of the mesh density control. Figure 3.1 shows the example of using of the automatic mesh density control.

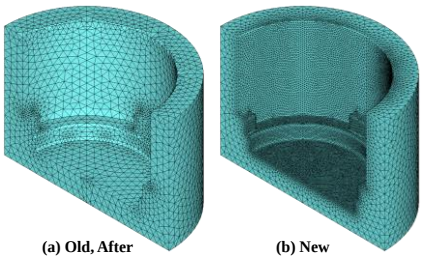

(a) Old, After (b) New

Figure 3.1 Mesh generation with automatic mesh density control

3.2 Temperature Input for Shrink Fit in Multi-body Analysis

Previously, the shrink fit analysis for dies was available during the multibody simulations, but the shrink fit connection between materials.

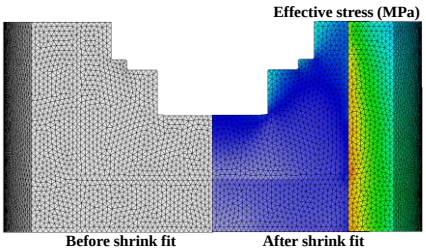

Figure 3.2 Shrink fit connection between instances in multi-body analysis (Temperature inputs)

Now, AFDEX_V21R03 provides the shrink fit analysis in multibody problems for each instance as described in Figure 3.2.

3.3 Friction Condition in Multi-body Analysis

Previously, only the Coulomb friction law has been used as the input for friction between the contacting bodies in Multibody analysis. In AFDEX_V21R03, constant shear friction law, hybrid friction law, etc. are added for various options of the friction condition. Figure 3.3 shows input UI design for the friction condition between the contacting bodies in multibody analysis.

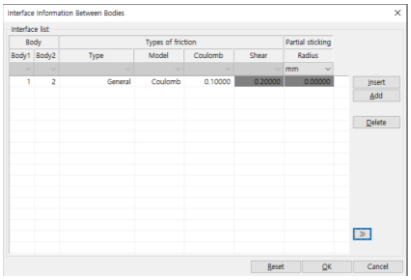

Figure 3.3 Input UI design for friction condition in multi-body simulation

3.4 Object Remeshing Feature in Multi-body Analysis

Previously, remeshing had been applied to whole objects or materials during finite element analyses of multibody structures or metal forming processes. AFDEX_V23 enables users to set the remeshing feature for each object. This feature can reduce the calculation time and improve the accuracy of the solution by selectively remeshing parts in the multibody analysis.

However, if it is necessary to use the remeshing due to the extreme distortion (Negative Jacobian) on finite elements during calculation, the remeshing is performed for the entire model.

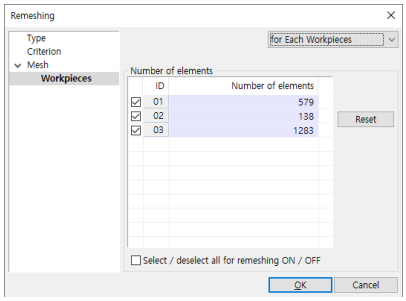

Figure 3.4 Object remeshing option dialog box

3.5 Improvement of Post-processor for multi-body Cases of Materials and Dies

AFDEX_V23 includes the plot with a legend for the number of nodes and elements for each die used for multi-body analysis. AFDEX_V21 and earlier versions had not provided this feature.

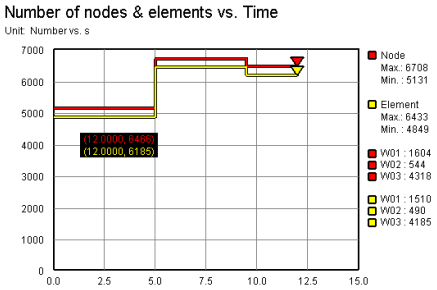

Figure 3.5 Improved UI for node/element information in multi-body analysis case

3.6 Result File Compression

During the simulation, the result file may become larger in size if the number of elements or steps stored is large. In order to solve this issue, AFDEX_V23 provides the selective save feature which lets users save the result data of desired solution steps. Various options to select the solution steps to be newly saved are prepared

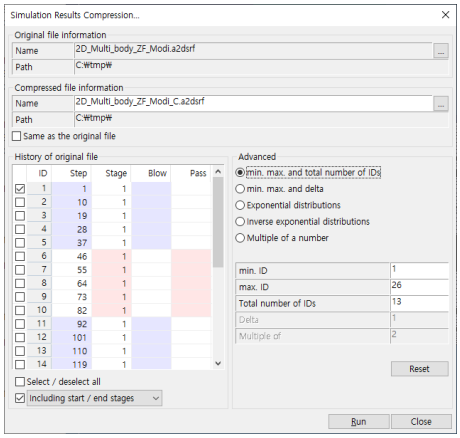

Figure 3.6 New UI of supporting selection of desired solution steps to be newly saved

3.7 UI for Inputting Translation Distance of Dies in Multi-stage Process Analysis

Multi-stage process analysis starts automatically after initializing the position of dies. If there are two or more dies for each upper and lower dies, there exists relative coordinates between the dies during the initialization step. The position of the dies at each stage should be determined because the dies position initialization is performed with the relative coordinates.

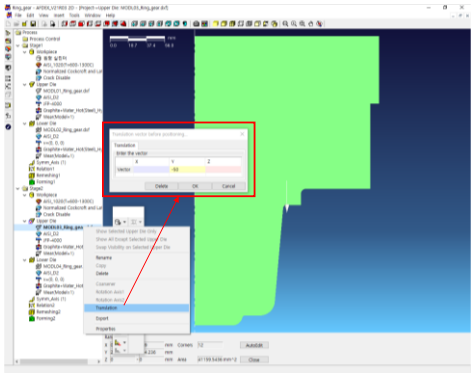

Figure 3.7 UI for inputting the translation distance of dies

AFDEX_V23 is designed in a way that run an analysis by entering a value of the translation distance of dies. In the case of the dies which are set up with this feature, the icon of a die part will be changed so that it can be distinguished from the original icon on AFDEX workspace window.

3.8 UI for Inputting Number of Elements for Remeshing in Die Structural Analysis

The mesh generation of dies is required for a die structural analysis, and high-density fine mesh can be used on a specific portion of dies. Generally, automatic mesh density control technique is applied on the die surface which is in contact with a workpiece, but user intervention can be necessary in case of special processes. Previously, input box for the number of elements of dies was included in the modeling dialog box, which was confusing for users to find it. AFDEX_V23 allows users to input data of a material or a value of the number of elements for each die in the Remeshing dialog box.

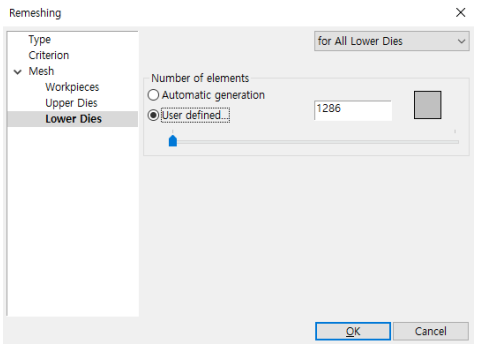

Figure 3.8 Dialog box of number of elements

3.9 Pre-processor Improvement for Shape Rolling Process Analysis

Previously, the basic input setting of the analysis condition is completed through the pre-processor of AFDEX, while the other inputs for specific conditions of the shape rolling process simulation such as the boundary conditions of rolls and materials were done by text file. For the convenience of use, AFDEX_V23 provides that all input data can be written in the pre-processor.

3.10 New Material Flow Models

Currently, AFDEX pre-processor provides 16 types of flow models including well-known traditional flow models (the Ludwik, Voce, Hollomon, and Swift equations) for formulating the flow curves. AFDEX_23 provides UI for 8 new flow models added in solver.

3.11 Pre-processor Improvement for Crack Analysis

Recently, crack analysis conditions suitable for 2D and 3D analysis and its solvers have been improved. Due to the change in the solvers, UI of pre-processor is also updated. The criteria for element removal in 2D and 3D crack analysis are as follows:

$$\text{2D: } w_1 D + w_2 \frac{\sigma_1}{\bar{\sigma}} + w_3 \frac{D\sigma_1}{\bar{\sigma}} + w_5 \frac{\dot{\bar{\varepsilon}}}{\dot{\bar{\varepsilon}}_{max}} > D_{cr}$$

$$\text{3D: } D > D_{cr} \;\&\; \dot{\bar{\varepsilon}} > \dot{\bar{\varepsilon}}_{cr} \;\&\; \dot{\bar{\varepsilon}} > w_5 \dot{\bar{\varepsilon}}_{max}$$

where D: damage, D_{cr}: critical damage, w_i: weight, $\bar{\sigma}$: yield stress, σ_1 : maximum principal stress, $\dot{\bar{\varepsilon}}$: effective strain rate, $\dot{\bar{\varepsilon}}_{max}$: Maximum effective strain rate.

3.12 Scale Tool for Material after Forming

Since hot forging product is formed with a heated material, thermal expansion becomes an important consideration for the process design. The material in the state where the current analysis has been completed is one that has been subjected to thermal expansion. In the previous version, it was not possible to check the shrinkage dimensional information of the material due to cooling after forming in the post-processor. AFDEX_V23 provides the checking feature for the size of the material that has been shrunk using the scale adjustment function through the post-processor.

4. Notice

4.1 Online Training in 2023

In response to the continued evolution of the COVID19 pandemic, all the training programs stand cancelled and MFRC is shifting in-person training to online training for applicants only.

Also, the tutorials and theories are uploaded on MFRC's YouTube channel. The following subjects will be provided: mathematical background, tensile testing, statics, solid mechanics, introduction to plasticity theory, finite strain, finite element method, and all materials related to metal forming, etc. Although the online lectures originally aim to help college students understand the materials, it can also be utilized as the materials introducing theories and mechanics used in AFDEX.

For more details, please refer to the link below.

(https://www.youtube.com/c/AFDEX)